

Received December 25, 2018, accepted January 14, 2019, date of publication January 21, 2019, date of current version February 8, 2019.

Digital Object Identifier 10.1109/ACCESS.2019.2893963

Monitoring Experiment of Electromagnetic Interference Effects Caused by Geomagnetic Storms on Buried Pipelines in China

ZEBANG YU¹, JIANHONG HAO², LIANGUANG LIU¹, AND ZEZHONG WANG²

¹State Key Laboratory of Alternate Electrical Power System with Renewable Energy Sources, North China Electric Power University, Beijing 102206, China

²North China Electric Power University, Beijing 102206, China

Corresponding author: Zebang Yu (yuzebang@126.com)

This work was supported in part by the National Key R&D Program of China under Grant 2016YFC0800100, in part by the National Natural Science Foundation of China under Grant 51577060, and in part by the Fundamental Research Funds for the Central Universities under Grant 2018QN018.

ABSTRACT The electromagnetic interference effects on buried pipelines induced by geomagnetic field are monitored for the first time in China, including geomagnetically induced current (GIC) and pipe-to-soil potential (PSP). It is of great significance for studying the influence of geomagnetic storms on pipeline corrosion and protection in mid–low latitudes. In order to monitor the GIC and PSP simultaneously, a monitoring experimental scheme is proposed. The monitoring data are obtained at Changyi oil transportation station (36°30'N, 119° 30'E) and Xiligu cathodic protection station (36°42'N, 119° 12'E). For comparison, the geoelectric field data are acquired from the geomagnetic observatory near the monitoring stations. Based on the monitoring result and theoretical consideration, the effectiveness of potentiostat and the influence of GIC on the pipeline is evaluated by analyzing the correlation between the monitoring data and the geoelectric field data. The monitoring data show that the pipeline GIC maximum is 7.88 A caused by the magnetic storm commencing suddenly and the PSP positive offset of the two monitoring points exceeds the limit required by relevant standards. The GIC maximum is 3.98 A caused by the magnetic storm commencing gradually, and the PSP offset exceeds the standard when the potentiostat is cut off. The results of our research indicate that the geomagnetic storms can also cause serious corrosion of pipelines in the middle and low latitudes; the larger the distance between insulating flanges is, the stronger the corrosion situation of pipelines will be; the greater the variation rate of geomagnetic disturbance is, the more serious the corrosion of pipelines will be. Because the protection range of the cathodic protection station is limited and the response performance of the potentiostats is varied in different areas, medium or small geomagnetic storms can also cause serious corrosion even if the pipeline is protected by the potentiostat.

INDEX TERMS Electromagnetic interference, petroleum industry, geomagnetism, magnetolectric effects, corrosion.

I. INTRODUCTION

The geomagnetic storm is caused by the solar wind under the action of the magnetosphere and the ionosphere [1], [2]. The buried pipelines are good conductors, according to electromagnetic induction law, the time-varying geomagnetic field generates an electric field in pipelines [3]. This field creates the geomagnetically induced current (GIC) through a loop formed by pipeline wall, pipeline grounding electrode, insulating coating, coating defects and the earth. GIC causes the pipe-to-soil potential (PSP) offset and leakage current in the coating defects. The leakage current causes the corrosion

rate increasing [4]. The mechanism of geomagnetic storms affecting buried pipeline is shown in Fig. 1.

The data of GIC and PSP are bases for evaluating the corrosion of pipelines as well as putting forward the protection strategies. Because the geomagnetic disturbance (GMD) of geomagnetic storms in high latitudes is stronger than that in middle and low latitudes, the research of the effect of GMD on buried pipelines began to be carried out in North America and Nordic countries firstly in 1978 [5]. Data of GIC and PSP have been obtained, the data analysis results show that GIC have a good correlation with the geoelectric field [6],

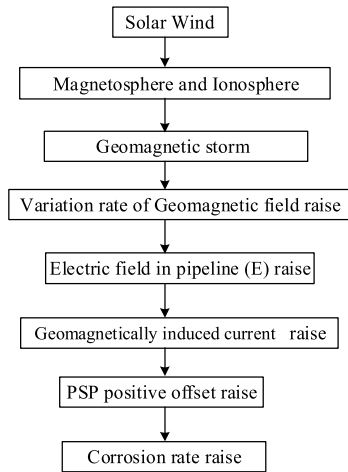


FIGURE 1. The mechanism of geomagnetic storms affecting the buried pipeline.

its magnitude is dependence on Earth conductivity structure [5], [7]. It can cause corrosion problems to the pipeline system, which bring large economic impacts particularly in high latitudes [7], [8]. The effect of the GIC on buried pipelines increases with the geomagnetic intensity increasing [9], [10]. Severe geomagnetic storms may lead to more severe corrosion of the pipeline with cathodic protection systems [11].

The corrosion rate of pipeline caused by GIC has been studied. The research results shown that GIC increases the PSP offset and corrosion rate. The cathodic protection current which maintains the pipeline at a constant potential ($-0.85V$) cannot protect the pipeline efficiently when sporadic large enhancements of GIC occurs [6]. The risk of corrosion can potentially reduce the safety performance and service life of the buried pipeline.

Boteler and Pulkkinen *et al.* have used the distributed source transmission line (DSTL) theory to calculate the GIC and PSP and obtained their distribution rule [4], [12]–[15]. The calculation results shown that the influence of GIC on oil and gas pipelines is related to length of the pipeline and the structure such as the corner and the branch points of the pipeline [13], [14]. In addition, the influence is also related to the geomagnetic intensity index (K_p), the larger the K_p is, the larger the influence will be [15].

However, the research of the effect of geomagnetic storms on pipelines is relatively less in the middle and low latitudes, Chinese scholars have investigated and compared the influence of geomagnetic storms affect to buried pipelines and power grids recently [16]–[18]. The monitoring data of GIC in 500 kV and 220 kV power grids in China have been acquired under geomagnetic storms in different intensity during July 2004 to December 2006. According to the GIC monitoring results, it can be seen that the GIC of 500 kV power grid is about 10 times larger than that of 220 kV power grid. The reason is that the smaller the DC resistance of the conductor is, the bigger the GIC which produced by the induction geoelectric field in the power grid will be. In Chinese 500 kV

power grid, the four-split conductors are generally used. In a unit length, the DC resistance of 500 kV power line is one fourth of that of 220 kV power line constituted by the single conductor. Therefore, the GIC of 500 kV power grid is larger than that of 220 kV power grid. The higher the voltage level is (in other words, the smaller the conductor resistance is), the greater the risk of power grid will be.

Based on the investigation of GIC in power grids, the interference of geomagnetic storms on pipelines is related to the structural factors of pipelines, such as the resistivity of insulation coating and the position and number of grounding electrodes of pipelines. But the monitoring data of GIC in pipelines have not been obtained, which are of great significance to evaluate the corrosion degree of the pipeline and optimize the restrain strategy of the corrosion.

Although the GMD in the middle and low latitudes is weaker than that in the high latitudes, the research findings of the GIC in power grids show that its influence exists in the power grids of China with the scale of power grids increasing [19]–[21]. The scale of oil and gas buried pipelines is increasing rapidly. The effects of geomagnetic storms on buried pipelines need to be studied, which is immediately connected with the safety and economic of oil and gas pipeline systems. In this paper we adopt a monitor scheme to acquire the data of GIC and PSP in pipelines. The GIC-PSP monitors have been installed in Changyi oil transportation station ($36^{\circ}30'N$, $119^{\circ}30'E$) and Xiligu cathodic protection station ($36^{\circ}42'N$, $119^{\circ}12'E$). Monitoring data are obtained during two geomagnetic storms. According to the comparison of the data acquired from two different monitoring stations of the same pipeline, the influence of geomagnetic storms on buried pipelines is investigated considering the variation rate of GMD, the output of potentiostats and the distance between insulation flanges.

II. MONITOR PRINCIPLE AND MONITOR SCHEME

A. MONITOR PRINCIPLE

The steel wall of the pipeline is protected by insulated coating, which is not directly contacted with the earth. Potentiostats are set up in cathodic protection stations and oil transportation stations to avoid corrosion caused by coating defects, which can be regarded as polarization power sources which providing compensation current (I_1) to keep the PSP below $-0.85V$ [22]. Because the electromagnetic environment of the pipelines is varying in different regions, output current and voltage of potentiostats is different. Insulation flanges are installed to the pipeline to realize the segment protection. When the pipeline does not need to be divided in the cathodic protection station, insulating flanges are still installed on the station, the two parts of pipeline can be protected by a potentiostat simultaneously using a jumper wire connecting the outsides of insulating flanges, the structure diagrammatic sketch of the cathodic protection station is shown in Fig. 2.

Since the frequency of GIC is with the range from $10^{-5}Hz$ to 1Hz [23], the current we monitored is a quasi-DC signal.

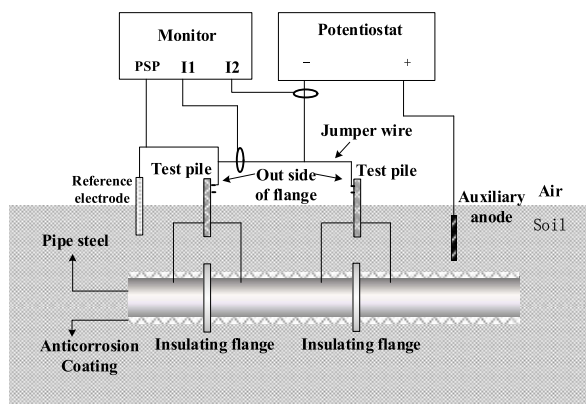


FIGURE 2. The structure diagrammatic sketch of the cathodic protection station and the installation of the GIC-PSP monitor.



FIGURE 3. The position of the two monitoring points of the pipeline.

According to the previous analysis, the current in pipeline (I_p) can be regarded as a superposition of two DC components, one of them is I_1 comes from the potentiostat and the other one is the GIC (I_2) induced by GMD of geomagnetic storms. So the GIC in the pipeline can be expressed as $I_2 = I_p - I_1$. The monitor we design has two current monitoring channels and one PSP monitoring channel. Two Hall sensors are used to collect the real-time data of I_1 and the current flow in the jumper wire (that is I_p), and the potential difference between the pipeline steel and the reference electrode (that is PSP) is collected at the same time. The diagrammatic sketch of the installation of the GIC-PSP monitor is shown in Fig. 2.

B. MONITOR SCHEME

Changyi oil transportation station is about 62 km away from the Bohai Sea. Xiligu cathodic protection station is 50 km away from the Bohai Sea. Both Changyi station and Xiligu station have potentiostats. Considering the intensity of GMD and the difficulty of installing detection instruments, these two stations are selected to install the GIC-PSP monitors, their locations are shown in Fig. 3.

The structure of the cathodic protection station and the installation of the monitor in Changyi station is same as Fig. 1. The preset output voltage of the potentiostat is -1.1V, which is different from the one in Xiligu station, -0.85V. There is no insulation flange at the both

sides of this station, so the GIC monitoring scheme using the jumper wire adopted in Changyi station cannot be implemented here. The acquisition of the current data need to be excavated. Because the influence range of the geomagnetic storm is global and the variation trend of the GIC in stations which is closed to each other is the same, the fluctuation trend of the GIC in Xiligu station can be characterized by that in Changyi station. We only monitor the PSP at this station because the PSP data is important to judge whether the drainage devices needs to be installed on pipeline. The monitor scheme of PSP in Xiligu station is the same as that in Changyi station.

III. DATA ANALYSIS

According to the monitoring scheme, the installation and commissioning of the monitoring equipment in Changyi station and Xiligu station are completed. The horizontal axis of monitoring data is universal time (UT).

A. GEOMAGNETIC STORM ON SEPTEMBER 7TH

The Dst index during 12:00 on September 7th to 00:00 on September 9th, 2017 is shown in Fig. 4 (a). In order to avoid the influence of geographical position and latitude on the data analysis, the electrical field data monitored by Anqiu Geomagnetic Observatory have been selected to compare with GIC and PSP. Anqiu Geomagnetic Observatory is the nearest station to the two pipeline monitoring stations. The relevant data are shown in Fig. 4. Fig. 4 (b) is the North-South component of the geoelectric field; Fig. 4 (c) is the East-West component of the geoelectric field; Fig. 4 (d) is the North-East component of the geoelectric field; Fig. 4 (e) is the GIC of Changyi station; Fig. 4 (f) is the PSP of Changyi station and Fig. 4 (g) is the PSP of Xiligu station.

1) ANALYSIS OF THE CORRELATION

Compared Fig. 4 (a) with (b), (c) and (d), it can be seen that the larger the Dst index decreases, the larger the fluctuation of the geoelectric field will be. Therefore, the rapid variation of the geoelectric field in Anqiu during 23:00 on the 7th to 00:00 on the 9th is caused by geomagnetic storm.

Compared the monitoring results of geoelectric field with the GIC, the fluctuation trend of the GIC coincides with that of the geoelectric field. The calculation formula of the correlation coefficients(r) of A and B can be written as:

$$r = \frac{\text{cov}(A, B)}{\sigma_A \sigma_B} \tag{1}$$

The $\text{cov}(A, B)$ is covariance of A and B , σ_A is the standard deviation of A , σ_B is the standard deviation of B . The correlation coefficients of the three components of the geoelectric field and the GIC is -0.64, 0.66 and 0.69, respectively, indicating that the GIC and the geoelectric field are correlated linearly. So the large fluctuation of the GIC during 23:00 on the 7th to 18:00 on the 8th is generated by the geomagnetic storm.

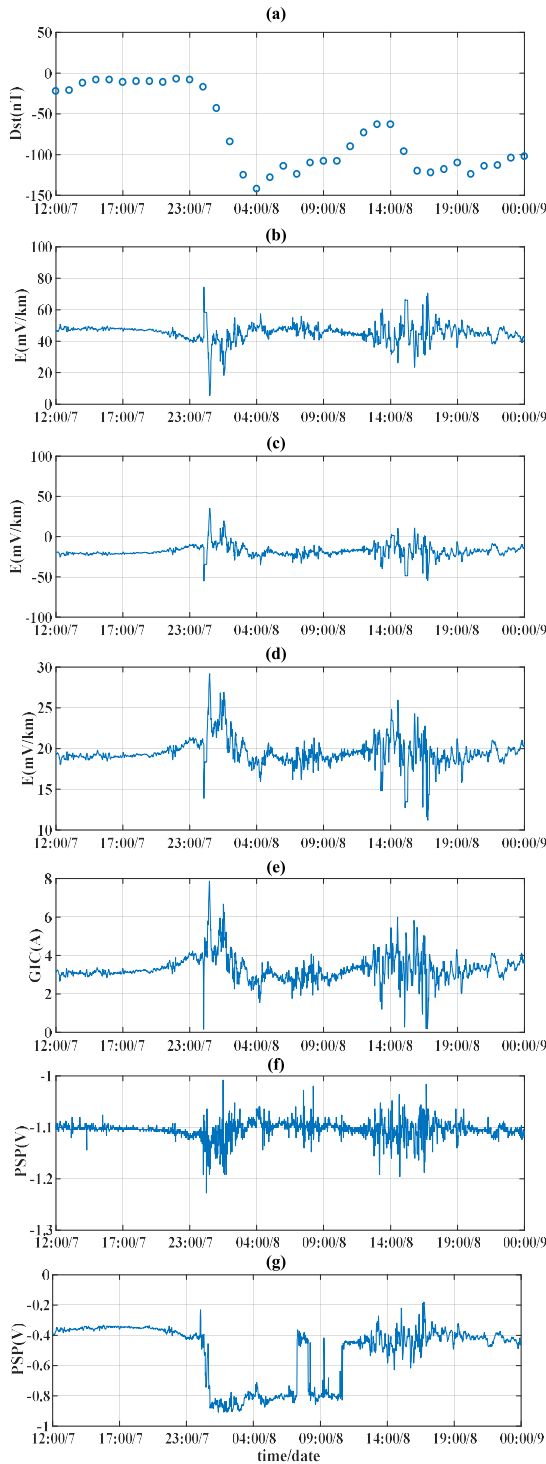


FIGURE 4. The Dst index and the monitoring results during 12:00 on September 7th to 00:00 on September 9th, 2017. (a) Dst index of 6th to 9th September. (b) North-South geoelectric field of Anqiu. (c) East-West geoelectric field of Anqiu. (d) North-East geoelectric field of Anqiu. (e) GIC in the pipeline of Changyi. (f) PSP in the pipeline of Changyi. (g) PSP in the pipeline of Xiligu.

Fig. 4 (e) and (f) show that the correlation between GIC and PSP of Changyi station is obvious, which indicates that GIC has a certain contribution to PSP. Fig. 4 (e) and (g) show

TABLE 1. Correlation coefficient of PSP and GIC in Xiligu station.

| Time | PSP | <i>r</i> |
|-----------------|----------------------|----------|
| 12:00/7-23:36/7 | switch-off potential | -0.99 |
| 23:36/7-06:03/8 | switch-on potential | -1.00 |
| 06:50/8-11:40/8 | switch-on potential | -1.00 |
| 11:40/8-00:00/9 | switch-off potential | -1.00 |

that the correlation between GIC of Changyi station and PSP of Xiligu station is not obvious. The reason of this monitoring result is that the potentiostat of Xiligu Station often stops working due to its faults, the PSP during faults of potentiostat is switch-off potential, and the PSP during normal operation of the potentiostat is switch-on potential. According to the faults time, the Xiligu PSP data is divided into four parts. The correlation coefficient (*r*) between Xiligu PSP data and Changyi GIC data of each part is calculated which is shown in table 1. The calculation results indicate that the PSP has a good correlation with GIC in each part.

2) ANALYSIS OF THE CHARACTERISTIC

The GIC value is stable around 3A without large fluctuation from 12:00 on 7th to 23:00 on 7th because the intension of GMD is small. With the Dst index declining rapidly from 23:00 on 7th to 04:00 on 8th, the GIC fluctuates intensely. The minimum and maximum values of GIC are 0.16A and 7.88A. During 04:00 to 13:00 on 8th, GIC tends to be stable with the descent velocity of Dst index decreases. With the increasing of the descent velocity of Dst index from 13:00 to 19:00, the fluctuation of GIC is large. It is illuminated that the GIC value is related to the descent velocity of Dst index. The larger the descent velocity of Dst index is, the larger the GIC will be.

The PSP of Changyi station is approximately stabilized at -1.1V from 12:00 on 7th to 23:00 on 7th. During 23:00 on 7th to 04:00 on 8th and 13:00 to 19:00 on the 8th, the PSP offset is large which have exceeded 100 mV many times. Reference [24] stipulates that DC current interference can be confirmed when PSP is positively offset by 20 mV. The drainage or other protective measures must be taken when PSP is positively offset by 100 mV. So the PSP offset beyond the limit which the drainage measures should be taken when the potentiostat working normally in Changyi station. It indicates that the pipelines near Changyi station have suffered a serious impact caused by geomagnetic storm. During 12:00 on 7th to 14:00 on 7th, the PSP has no obvious fluctuation in Xiligu station, but the offset of PSP is large during 23:00 on the 7th to 00:00 on the 9th. Especially during the faults time of potentiostat from 13:00 to 19:00 on 8th, the PSP offset exceeds 100mV many times. The power-off operations of the potentiostat can also cause the PSP offset whose magnitude is larger than that caused by geomagnetic storms.

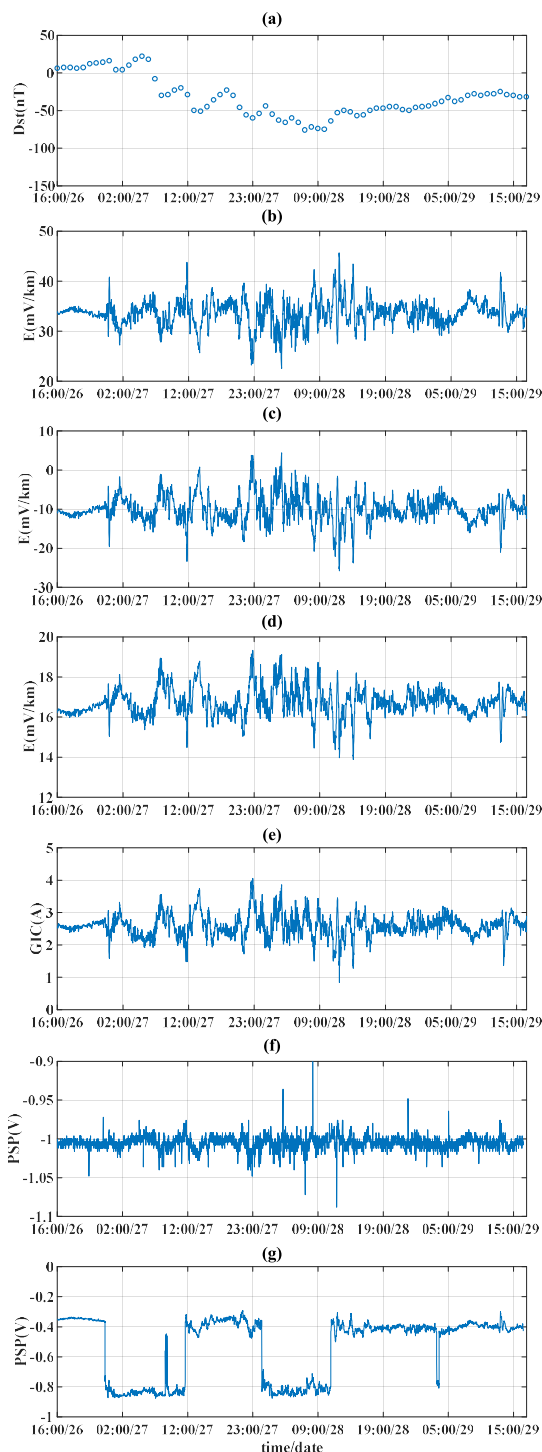


FIGURE 5. The Dst index and the monitoring results during 16:00 on September 26th to 15:00 on September 29th, 2017. (a) Dst index of 26th to 29th September. (b) North-South geoelectric field of Anqiu. (c) East-West geoelectric field of Anqiu. (d) North-East geoelectric field of Anqiu. (e) GIC in the pipeline of Changyi. (f) PSP in the pipeline of Changyi. (g) PSP in the pipeline of Xiligu.

B. GEOMAGNETIC STORM ON SEPTEMBER 26TH

During September 26th to 29th, 2017, the Dst index, Anqiu geoelectric field, GIC of Changyi pipeline, PSP of Changyi station and PSP of Xiligu station are shown in Fig. 5.

TABLE 2. Correlation coefficient of PSP and GIC in Xiligu station.

| Time | PSP | <i>r</i> |
|-------------------|----------------------|----------|
| 16:00/26-23:12/26 | switch-off potential | -0.91 |
| 23:12/26-11:35/27 | switch-on potential | -0.74 |
| 11:35/27-00:21/28 | switch-off potential | -0.95 |
| 00:21/28-10:53/28 | switch-on potential | -0.67 |
| 10:53/28-03:07/29 | switch-off potential | -0.94 |
| 03:26/29-16:00/29 | switch-off potential | -0.95 |

1) ANALYSIS OF THE CORRELATION

Fig. 5 (a), (b), (c) and (d) show that, the amplitude of the geoelectric field is highly correlated with the declining rate of Dst index. Compared Fig. 5 (b), (c) and (d) with (e), it can be seen that the fluctuation trend of the GIC is related to the geoelectric field. The linear correlation coefficients of the GIC and the three components of the geoelectric field is -0.87 , 0.89 and 0.87 respectively. It is indicated that the GIC in pipeline is caused by the geomagnetic storm. The Fig. 5 (e) and (f) show that, the GIC has a certain contribution to the PSP. According to the power-off time of the potentiostat in Xiligu station, the PSP data of Xiligu are divided to six parts. The linear correlation coefficient (*r*) between PSP and GIC in each part is shown in table 2, which indicates that the PSP has a good correlation with GIC.

2) ANALYSIS OF THE CHARACTERISTIC

From 07:00 on 27th to 19:00 on 28th, the minimum value of the GIC is 0.84A and the maximum value was 3.98A, which is lower than that of geomagnetic storm on 8th. It is because the descent velocity of Dst index is lower during this geomagnetic storm.

From 07:00 on 27th to 19:00 on 28th, the PSP value of the pipeline in Changyi Station is stable around $-1V$. The offset of the PSP is less than 100 mV indicating that there is no need to take the drainage or other protective measures during this time. During the normal operation of potentiostat in Xiligu station, the PSP offset is low, the maximum positive offset is 98 mV. However, during the power-off operation of potentiostat, the PSP positive offset exceeds 100mV many times. This monitoring result indicates that, although the influence of geomagnetic storms can be effectively restrained by potentiostat in the middle or small geomagnetic storms, the pipeline still suffers a serious effect produced by GIC during the power-off time of the potentiostat. This effect will be more serious in the pipeline far away from the cathodic protection station, because the output current (I_1) cannot protect the pipeline efficiently there. So the drainage measures are still needed during the middle and small geomagnetic storms.

IV. THEORETICAL CONSIDERATION

According to the Plane Wave Theory [25], the relationship of the electrical field in pipeline and the variation rate of the

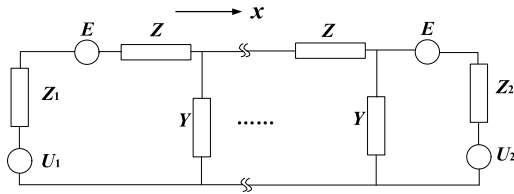


FIGURE 6. The equivalent circuit model of buried pipeline.

geomagnetic field (dB/dt) is as follow:

$$E(t) = -\frac{1}{\sqrt{\pi\mu_0\sigma}} \int_{-\infty}^t \frac{g(u)}{\sqrt{t-u}} du \quad (2)$$

where $E(t)$ is the induced electrical field in pipeline, μ_0 is the vacuum permeability, σ is the ground conductivity, $g(t)$ is the variation rate of the geomagnetic field, dB/dt .

According to the Distributed Source Transmission Line (DSTL) theory [4], the pipeline is equivalent to a lot of T-type circuits in series as shown in Fig. 6. The induced electric field of pipeline (E) is equivalent to a voltage source in each section. The calculation method of the distribution of GIC and PSP can be obtained as follow:

$$I(x) = -\frac{EL}{Z_1 + Z_2} + \frac{U_1 - U_2}{Z_1 + Z_2} \quad (3)$$

$$U(x) = E \left(x - \frac{LZ_1}{Z_1 + Z_2} \right) + \frac{U_1Z_2 - U_2Z_1}{Z_1 + Z_2} \quad (4)$$

where the I is GIC; U is PSP; E is the electrical field in pipeline; L is the length of the pipeline; Z_1 and Z_2 is the terminated impedance of the pipeline; U_1 and U_2 is the terminated voltage source of the pipeline.

According to (2) the $E(t)$ is proportional to $-dB/dt$. The (3) and (4) reveals that the larger the E is, the larger the GIC and PSP will be. So the corrosion rate of pipelines during the geomagnetic storm is related to $-dB/dt$, the $-dB/dt$ is the same to the descent velocity of Dst index.

Compared the PSP values of the two monitoring stations from 00:00 to 07:00 on the 8th, it is found that the PSP offset in Xiligu station is larger than that in Changyi station. In order to research this phenomenon, the operation of the potentiostats, the difference of geological structure and the structure parameters of the pipeline have been considered. In this period the potentiostat operates normally and there is no difference of geological structure between these two stations. So the influence of the potentiostat and the geoelectric structure on the monitoring results can be ignored.

To ensure the pipeline operates safety, insulation flanges are installed in Weixian valve room, Wenhexi valve room and Weihedong valve room, the locations of the insulation flanges are shown in Fig. 3. So the pipeline has been divided into three parts (A, B, C) and there is no electrical connection between them. The length (L_i) of each part as well as the clockwise angle (θ) between the pipeline and due South are obtained and shown in table 3. According to the DSTL theory, the distribution of PSP along the part A containing the Xiligu station have been calculated as shown in Fig. 7 (a),

TABLE 3. The length of pipelines and the angle between the pipelines and the East direction.

| Pipeline section | A | B | C |
|------------------|--------|--------|--------|
| θ | 45.85° | 45.85° | 68.77° |
| L_i | 22 km | 5 km | 8 km |

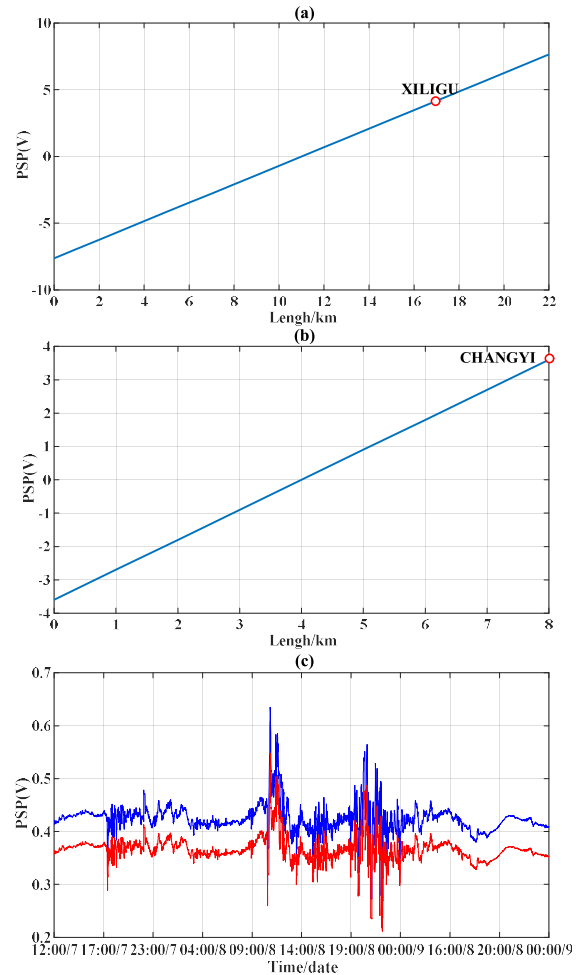


FIGURE 7. (a) PSP distribution along part A, (b) PSP distribution along part C, (c) PSP calculation values in Xiligu station (blue) and Changyi station (red).

on the assumption that the geoelectric field is 1 mV/km. The distribution of PSP along the part C containing the Changyi station is shown in Fig. 7 (b).

According to the calculation results, the time-varying PSP of Xiligu station and that of Changyi station have been calculated during the geomagnetic storm from 12:00 on the 7th to 00:00 on the 9th and the calculation result is shown in Fig. 7 (c). Comparison between Fig. 7 (a) and Fig. 7 (b), it can be revealed that the PSP offset increases with the length of the pipeline increasing during the geomagnetic storm. The distance between the insulation flanges on the both sides of Xiligu station is longer than that of Changyi station, so the PSP offset of Xiligu station is larger than that of Changyi station as shown in Fig. 7 (c). This result indicates

that, during the geomagnetic storms, the longer the distance between insulating flanges is, the larger the PSP offset will be. So the corrosion rate of pipelines during geomagnetic storm on pipeline is related to distance between insulating flanges.

The output current of the potentiostat flows from auxiliary anode (a kind of metal more active than steel) to pipeline steel to compensate for the loss of electrons at coating defects. Its output voltage is set up to ensure the PSP stable in an ideal range. When the potentiostat is power off, the PSP will be elevated to the nature potential which is more positive than the preset potential and the electric current density will be enlarged. Therefore, during the geomagnetic storms, the corrosion rate is related not only to the GIC in pipelines, but also to the operation of potentiostats.

V. CONCLUSION

In this paper, the monitoring data of GIC in the buried pipeline generated by geomagnetic storms are acquired for the first time in the middle and low latitude countries. The monitoring data of PSP are obtained simultaneously. Based on data analysis and the theoretical consideration, the main conclusions of this paper are as follows.

(1) During the geomagnetic storm, the PSP positive offset of the pipelines can exceed the limit of the technical standard for DC interference mitigation of buried pipeline, which revealed that the geomagnetic storm can effect on buried pipelines in the middle and low latitudes. Although the intensity of GMD in the middle and low latitudes countries is weaker than that in high latitudes countries during the geomagnetic storm, the coating defects and the potentiostat faults operation cannot be avoided. So it is of great significance to investigate the effect caused by GMD of geomagnetic storm on buried pipelines in middle and low latitudes countries.

(2) The effective control of potentiostats can restrain the corrosion of pipelines near the cathodic protection stations during the medium or small geomagnetic storms, but the response performance and the effective protection distance of potentiostats are greatly varied in different areas due to the geoelectric structure difference and the electromagnetic environment difference. In addition, the protection range of the cathodic protection station is limited. The farther the pipeline from potentiostat is, the smaller the effect of cathodic protection will be, which is explained in the appendix. When the potentiostat fails in responding or the pipeline exceeds the effective protection range, medium or small geomagnetic storms can also cause serious corrosion. With the scale of the buried pipelines increasing, it is suggested that the study on the prevention strategies of the corrosion caused by geomagnetic storm should be started as soon as possible.

(3) The impact of geomagnetic storms on pipelines is related to the environmental factors such as latitude and longitude, geoelectric structure and Kp index. Moreover, it is also related to factors such as the variation rate of the geomagnetic field and the distance between the insulation flanges, the longer the distance between the insulation flanges is, the larger the effect of GIC on buried pipeline will be.

It is suggested that the distribution of insulating flange should be optimized to restrain the effect of geomagnetic storm on the pipeline corrosion. In order to understand the effect of various factors on corrosion, the investment of the monitoring experiments will be huge with the scale of pipelines becoming larger and larger. So it is necessary to study and establish the theoretical evaluation system for the influence of various factors on pipeline corrosion.

APPENDIX

The output current of the potentiostat changes according to the different value of PSP which is the potential difference between pipeline and the reference electrode. This current can compensate the lost electrons at the coating defects. Therefore, the potentiostat can be regarded as a dynamic DC source. The circuit model of the pipeline with a potentiostat ignoring the effects of other interference sources is shown in Fig. 8.

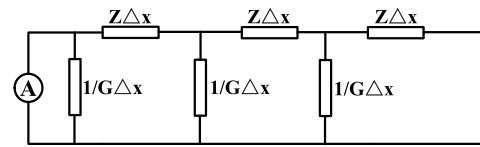


FIGURE 8. The circuit model of the pipeline with a potentiostat.

According to Fig. 8 and Kirchhoff law, only take the potentiostat output into account, the current (I_1) in the pipeline is:

$$[I_1(x - \Delta x) - I_1(x)] \cdot \frac{1}{G\Delta x} = I_1(x) Z\Delta x + [I_1(x) - I_1(x + \Delta x)] \cdot \frac{1}{G\Delta x} \quad (5)$$

The Δx is the calculation step. It can be obtained that:

$$I_1(x) = C_1 e^{\sqrt{ZG}x} + C_2 e^{-\sqrt{ZG}x} \quad (6)$$

$$C_1 = I_0 - \frac{I_0 - ZGI_0\Delta x^2 - I_0 e^{\sqrt{ZG}}}{e^{-\sqrt{ZG}} - e^{\sqrt{ZG}}} \quad (7)$$

$$C_2 = \frac{I_0 - ZGI_0\Delta x^2 - I_0 e^{\sqrt{ZG}}}{e^{-\sqrt{ZG}} - e^{\sqrt{ZG}}} \quad (8)$$

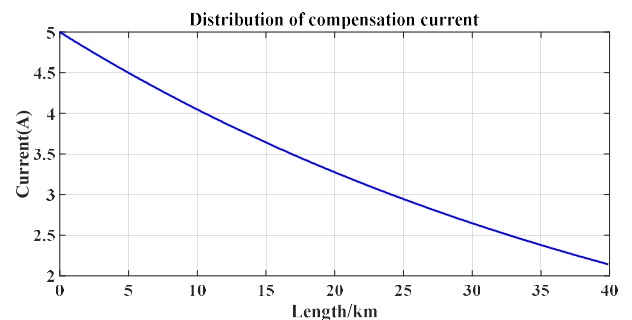


FIGURE 9. The compensation current distribution along the pipeline.

I_0 is the output current of the potentiostat. According to (6), on the assumption that I_0 is 5A, the distribution of the compensation current along a 40km pipeline at can be calculated as shown in Fig. 9, the potentiostat is at the starting point.

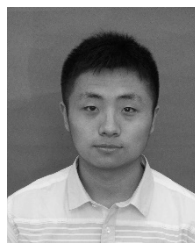
Fig. 9 shows that the compensation current reduces with the distance between the pipeline and the potentiostat increasing. So the farther the pipeline from potentiostat is, the smaller the effect of cathodic protection will be.

ACKNOWLEDGMENT

The authors would like to thank the Institute of Earthquake Forecasting, CEA for providing geoelectric field data, and the World Data Center for Geomagnetism, Kyoto (WGC) which provided the value of the Dst index.

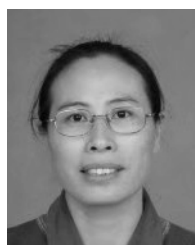
REFERENCES

- [1] S. V. Avakyan and N. A. Voronin, "The role of cosmic and ionospheric disturbances in global climatic changes and pipeline corrosion," *Izvestiya, Atmos. Ocean. Phys.*, vol. 47, no. 9, pp. 1143–1158, Dec. 2011.
- [2] S. V. Avakyan and A. A. Namgaladze, "Some technospheric manifestations of heliogeophysical disturbances," *Herald Russian Acad. Sci.*, vol. 82, no. 1, pp. 63–68, Feb. 2012.
- [3] R. Pirjola, "Geomagnetically induced currents during magnetic storms," *IEEE Trans. Plasma Sci.*, vol. 28, no. 6, pp. 1867–1873, Dec. 2000.
- [4] A. Pulkkinen, R. Pirjola, D. Boteler, A. Viljanen, and I. Yegorov, "Modelling of space weather effects on pipelines," *J. Appl. Geophys.*, vol. 48, no. 4, pp. 233–256, Dec. 2001.
- [5] W. H. Campbell, "Induction of auroral zone electric currents within the Alaska pipeline," *Pure Appl. Geophys.*, vol. 116, no. 6, pp. 1143–1173, 1978.
- [6] A. Osella, A. Favetto, and E. López, "Currents induced by geomagnetic storms on buried pipelines as a cause of corrosion," *J. Appl. Geophys.*, vol. 38, no. 3, pp. 219–233, Jun. 1997.
- [7] R. Pirjola, A. Viljanen, A. Pulkkinen, and O. Amm, "Space weather risk in power systems and pipelines," *Phys. Chem. Earth, C, Sol., Terr. Planet. Sci.*, vol. 25, no. 4, pp. 333–337, Sep. 2000.
- [8] P. Hejda and J. Bochníček, "Geomagnetically induced pipe-to-soil voltages in the Czech oil pipelines during October–November 2003," *Annales Geophysicae*, vol. 23, no. 9, pp. 3089–3093, Nov. 2005.
- [9] A. Favetto and A. Osella, "Numerical simulation of currents induced by geomagnetic storms on buried pipelines: An application to the Tierra del Fuego, Argentina, gas transmission route," *IEEE Trans. Geosci. Remote Sens.*, vol. 31, no. 1, pp. 614–619, Jan. 1999.
- [10] R. A. Gummow and P. Eng, "GIC effects on pipeline corrosion and corrosion control systems," *J. Atmos. Solar-Terr. Phys.*, vol. 64, no. 16, pp. 1755–1764, 2002.
- [11] M. Ingham and C. J. Rodger, "Telluric field variations as drivers of variations in cathodic protection potential on a natural gas pipeline in New Zealand," *Space Weather*, vol. 16, no. 9, pp. 1396–1409, Sep. 2018.
- [12] D. H. Boteler and M. J. Cookson, "Telluric currents and their effects on pipelines in the Cook Strait region of New Zealand," *Mater. Perform.*, vol. 25, no. 3, pp. 27–32, 1986.
- [13] D. H. Boteler, R. J. Pirjola, and H. Nevanlinna, "The effects of geomagnetic disturbances on electrical systems at the Earth's surface," *Adv. Space Res.*, vol. 22, no. 1, pp. 17–27, Nov. 1998.
- [14] D. H. Boteler, "Geomagnetic effects on the pipe-to-soil potentials of a continental pipeline," *Adv. Space Res.*, vol. 26, no. 1, pp. 15–20, 2000.
- [15] D. H. Boteler, "A new versatile method for modelling geomagnetic induction in pipelines," *Geophys. J. Int.*, vol. 193, no. 1, pp. 98–109, Apr. 2012.
- [16] P. Zhang, L. Liu, and C. Ma, "Comparison of geomagnetic storm interference in pipelines and power system," *Sci. Technol. Eng. (in Chin.)*, vol. 15, no. 25, Sep. 2015.
- [17] L.-G. Liu, C.-M. Liu, B. Zhang, Z.-Z. Wang, X.-N. Xiao, and L.-Z. Han, "Strong magnetic storm's influence on China's Guangdong power grid," *Chin. J. Geophys.*, vol. 51, no. 4, pp. 694–699, Jul. 2008.
- [18] L. Liu, P. Zhang, K. Wang, W. Bi, and A. Ge, "PSP Interference Effect of Geomagnetic Storm on Buried Pipelines," *Trans. China Electrotech. Soc. (in Chin.)*, vol. 31, no. 9, pp. 68–74, May 2016.
- [19] L.-G. Liu, K. Wei, and X.-N. Ge, "GIC in future large-scale power grids: An analysis of the problem," *IEEE Electr. Mag.*, vol. 3, no. 4, pp. 52–59, Dec. 2015.
- [20] C.-M. Liu, L.-G. Liu, and R. Pirjola, "Geomagnetically induced currents in the high-voltage power grid in China," *IEEE Trans. Power Del.*, vol. 24, no. 4, pp. 2368–2374, Oct. 2009.
- [21] C.-M. Liu, L.-G. Liu, R. Pirjola, and Z.-Z. Wang, "Calculation of geomagnetically induced currents in mid- to low-latitude power grids based on the plane wave method: A preliminary case study," *Space Weather*, vol. 7, no. 4, pp. 1–9, Apr. 2009.
- [22] S. Croall, "Cathodic protection remote monitoring for a gas distribution system," *Mater. Perform.*, vol. 36, no. 7, Jul. 1997.
- [23] D. H. Boteler and L. Trichtchenko, "A common theoretical framework for AC and telluric interference on pipelines," in *Proc. NACE CORROSION, Symp.*, 2005, Art. no. 05614.
- [24] *Technical standard for DC interference mitigation of buried pipeline.*, Standard, GB 50991-2014, 2014.
- [25] A. Viljanen and R. Pirjola, "Geomagnetically induced currents in the Finnish high-voltage power system," *Surv. Geophys.*, vol. 15, no. 4, pp. 383–408, Jul. 1994.



ZEBANG YU was born in Songyuan, China, in 1989. He received the B.S. degree in automation specialty from the Institute of Technology of Tianjin, in 2012, and the M.S. degree in electrical engineering from Northeastern University, Shenyang, China, in 2014. He is currently pursuing the Ph.D. degree in electrical engineering with North China Electric Power University, Beijing, China.

Since 2015, he has been with the State Key Laboratory of Alternate Electrical Power System with Renewable Energy Sources, North China Electric Power University. His research interests include control and analysis in power system operation, power system monitoring and mitigation, modeling geomagnetically induced currents in the oil and gas pipelines, and assessing the effect on buried pipeline systems.



JIANHONG HAO was born in Shijiazhuang, in 1960. She received the Ph.D. degree in plasma specialty from the Chinese Academy of Engineering Physics, in 2003. She is currently a Professor, a Doctoral Supervisor, and the Director of the Institute of Modern Electronic Technology, North China Electric Power University. She is mainly involved in teaching and research in the fields of physical electronics and electromagnetic field and microwave technology, and she has researched

experience in the fields of high-power microwave theory, microwave source technology, and beam–beam interaction of strong radiation for many years. She has taken the lead in the research of nonlinear phenomena in high-power microwave sources in China and achieved the remarkable results.



LIANGUANG LIU was born in Jilin, China, in 1954. He received the M.Sc. degree in electrical engineering from North China Electric Power University (NCEPU), Beijing, China, in 1994, where he has been a Professor and a Doctoral Supervisor with the School of Electrical and Electronic Engineering. His research interests have included safe operation and hazard prevention of power systems and power quality. He is a Senior Member of the Chinese Society for Electrical Engineering.

He is a Commissioner of the Chinese Space Weather Committee and the National Space Weather Monitoring and Pre-Warning Technology Standard Committee.



ZEZHONG WANG was born in Shandong, China, in 1960. He received the B.Eng., M.Eng., and Ph.D. degrees in electrical engineering from Tsinghua University, in 1983, 1986, and 1989, respectively. He is currently a Professor and a Doctoral Supervisor with the School of Electrical and Electronic Engineering, North China Electric Power University. His research interests include electromagnetic field numerical analysis, electromagnetic compatibility, and electromagnetic measurement.

• • •